



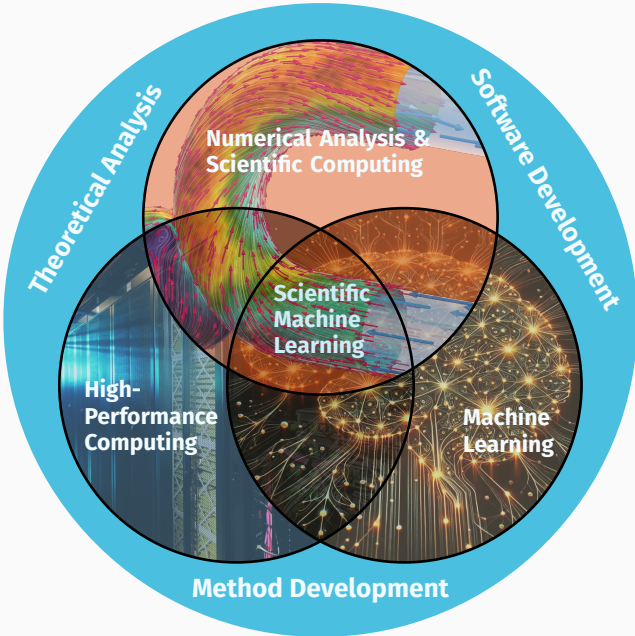
Some Algorithmic Advances in Cardiovascular Simulations

Alexander Heinlein¹

Interdisciplinary Aneurysm Science Workshop (IASW2025), July 29, 2025

¹Delft University of Technology

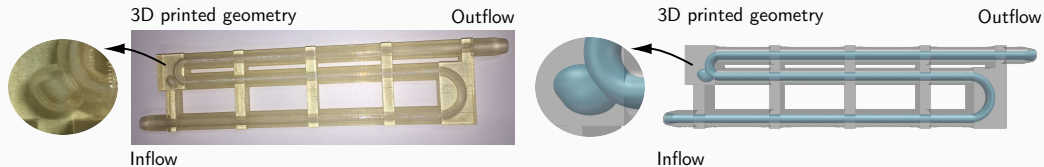
SCaLA – Scalable Scientific Computing and Learning Algorithms



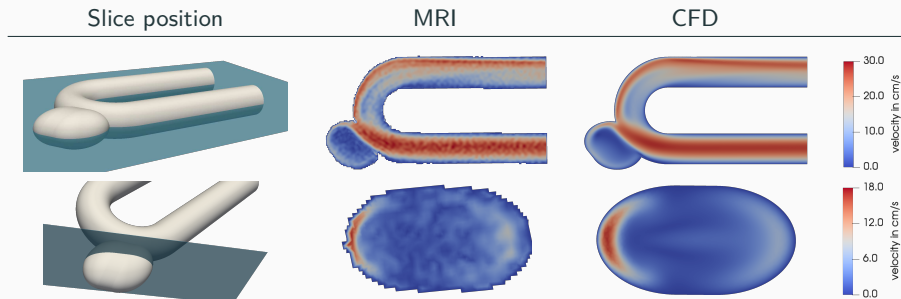
Surrogate models for aneurysm simulations

Computational Fluid Dynamics (CFD) Simulations are Time Consuming

In Giese, Heinlein, Klawonn, Knepper, Sonnabend (2019), a benchmark for comparing MRI measurements and CFD simulations of hemodynamics in **intracranial aneurysms** was proposed.

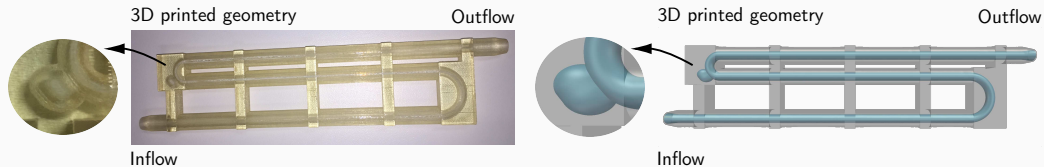


To obtain accurate simulation results, a simulation with $\approx 10^6$ d.o.f.s has been carried out. On $O(100)$ MPI ranks, the computation of a steady state took $O(1)$ h on CHEOPS supercomputer at UoC.

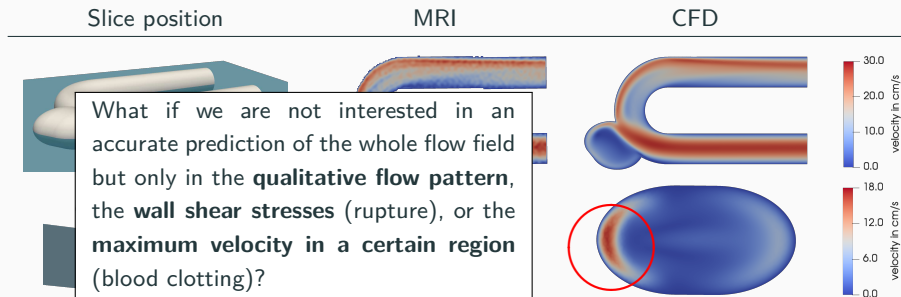


Computational Fluid Dynamics (CFD) Simulations are Time Consuming

In Giese, Heinlein, Klawonn, Knepper, Sonnabend (2019), a benchmark for comparing MRI measurements and CFD simulations of hemodynamics in **intracranial aneurysms** was proposed.



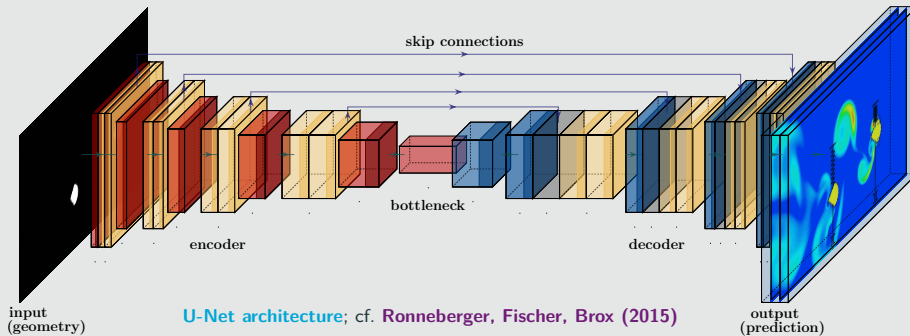
To obtain accurate simulation results, a simulation with $\approx 10^6$ d.o.f.s has been carried out. On $O(100)$ MPI ranks, the computation of a steady state took $O(1)$ h on CHEOPS supercomputer at UoC.



Convolutional Neural Network-Based Surrogate Model

CNN-based approach

We employ a **convolutional neural network (CNN)** (**LeCun (1998)**) to predict the stationary flow field, given an **image of the geometry as input**.



Related works (non-exhaustive)

- **Guo, Li, Iorio (2016)**
- **Niekamp, Niemann, Schröder (2022)**
- **Stender, Ohlsen, Geisler, Chabchoub, Hoffmann, Schlaefer (2022)**

Operator learning (non-exhaustive)

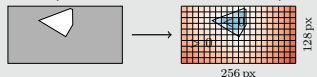
- **FNOs:** Li et al. (2021)
- **PCA-Net:** Bhattacharya et al. (2021)
- **Random features:** Nelsen and Stuart (2021)
- **CNOs:** Raonić et al. (2023)

Comparison OpenFOAM® Versus CNN (Relative Error 2 %)

We automatically generate geometries and compute the corresponding flow fields using OPENFOAM®.

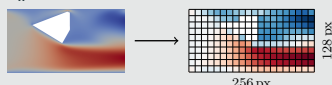
Input data

SDF (Signed Distance Function)

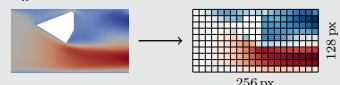


Output data

u_x



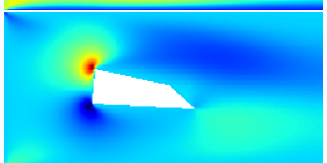
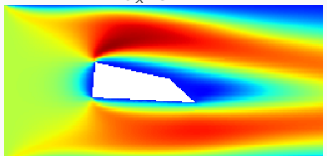
u_x



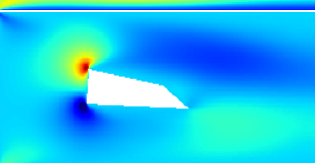
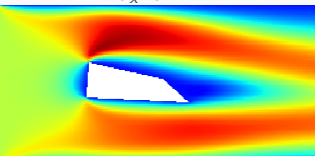
u_x CFD

u_x CNN

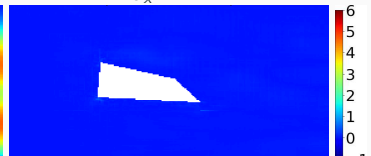
u_x ERR



u_y CFD



u_y CNN



u_y ERR



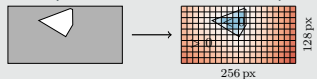
Cf. Eichinger, Heinlein, Klawonn (2021, 2022).

Comparison OpenFOAM® Versus CNN (Relative Error 14 %)

We automatically generate geometries and compute the corresponding flow fields using OPENFOAM®.

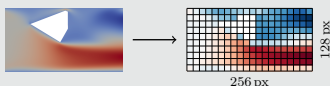
Input data

SDF (Signed Distance Function)

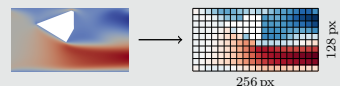


Output data

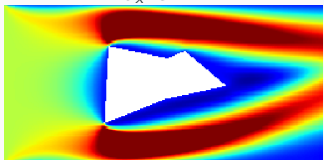
u_x



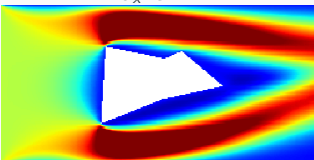
u_x



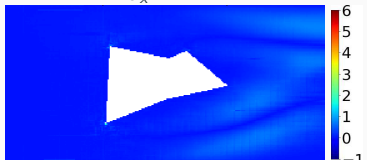
u_x CFD



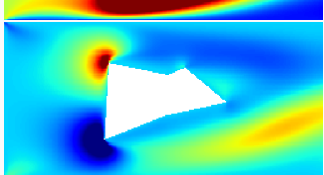
u_x CNN



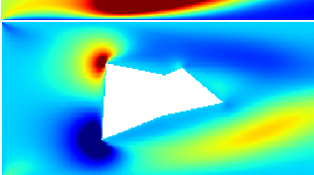
u_x ERR



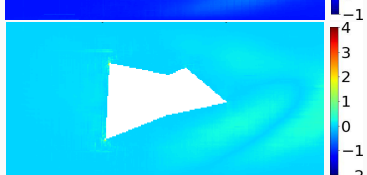
u_y CFD



u_y CNN



u_y ERR



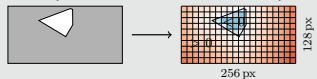
Cf. Eichinger, Heinlein, Klawonn (2021, 2022).

Comparison OpenFOAM® Versus CNN (Relative Error 31 %)

We automatically generate geometries and compute the corresponding flow fields using OPENFOAM®.

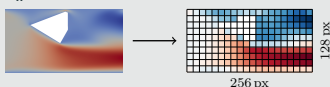
Input data

SDF (Signed Distance Function)

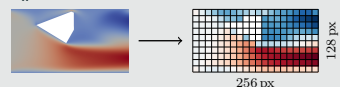


Output data

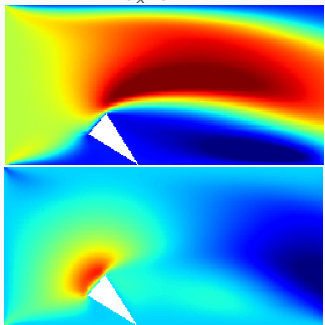
u_x



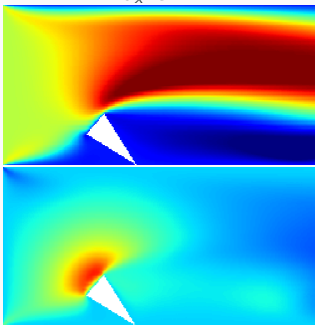
u_x



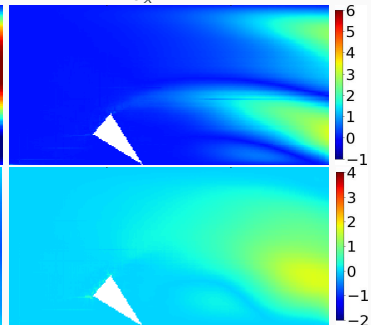
u_x CFD



u_x CNN



u_x ERR



u_y CFD

u_y CNN

u_y ERR

Cf. Eichinger, Heinlein, Klawonn (2021, 2022).

Computing Times

Data generation:

avg. runtime per case (serial)	
create STL	0.15 s
snappyHexMesh	37 s
simpleFoam	13 s
total time	≈ 50 s

Training:

U-Net		
# decoders	1	2
# parameters	≈ 34 m	≈ 53.5 m
time/epoch	195 s	270 s

Comparison CFD Vs NN:

OPENFOAM®	U-Net	
CPU	CPU	GPU
avg. time	50 s	0.092 s

⇒ Flow predictions using neural networks may be less accurate and the **training phase expensive**, but the **flow prediction is $\approx 5 \cdot 10^2 - 10^4$ times faster**.

Unsupervised Learning Approach – PDE Loss Using Finite Differences

Physics-informed loss function

We train the CNN by incorporating the squared PDE residuals into the **loss function**:

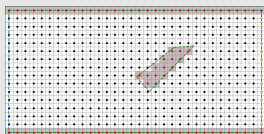
$$\mathcal{L}_{\text{PDE}} = \frac{1}{N_{\text{PDE}}} \sum_{i=1}^{N_{\text{PDE}}} \|\mathcal{R}(u_{\text{CNN}}, p_{\text{CNN}})\|^2$$

Here, N_{PDE} is the number of training configs.

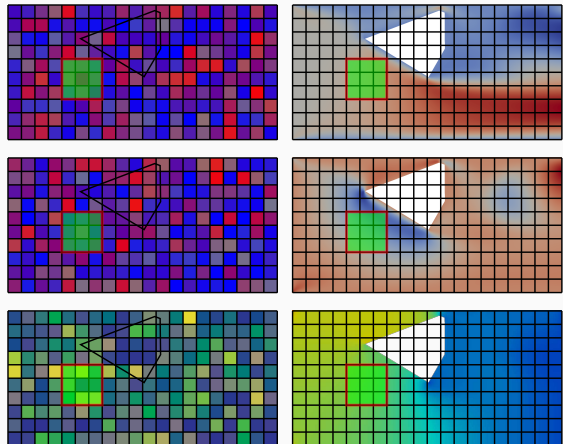
Cf. [Raissi et al. \(2019\)](#), [Dissanayake and Phan-Thien \(1994\)](#), [Lagaris et al. \(1998\)](#).

We discretize the differential operators using finite differences on the output pixel image.

Boundary conditions



We explicitly enforce boundary conditions on the output image → **hard constraints**



$$\|\mathcal{R}(u_{\text{CNN}}, p_{\text{CNN}})\|^2 >> 0 \quad \|\mathcal{R}(u_{\text{CNN}}, p_{\text{CNN}})\|^2 \approx 0$$

Here, we consider the **Navier–Stokes equations**:

$$\mathcal{R}(u_{\text{CNN}}, p_{\text{CNN}}) = \begin{bmatrix} -\nu \Delta \vec{u} + (\vec{u} \cdot \nabla) \vec{u} + \nabla p \\ \nabla \cdot \vec{u} \end{bmatrix}$$

Cf. [Grimm, Heinlein, Klawonn \(2025\)](#).

Results on $\approx 5\,000$ Geometries – Data-Based Versus Physics-Informed

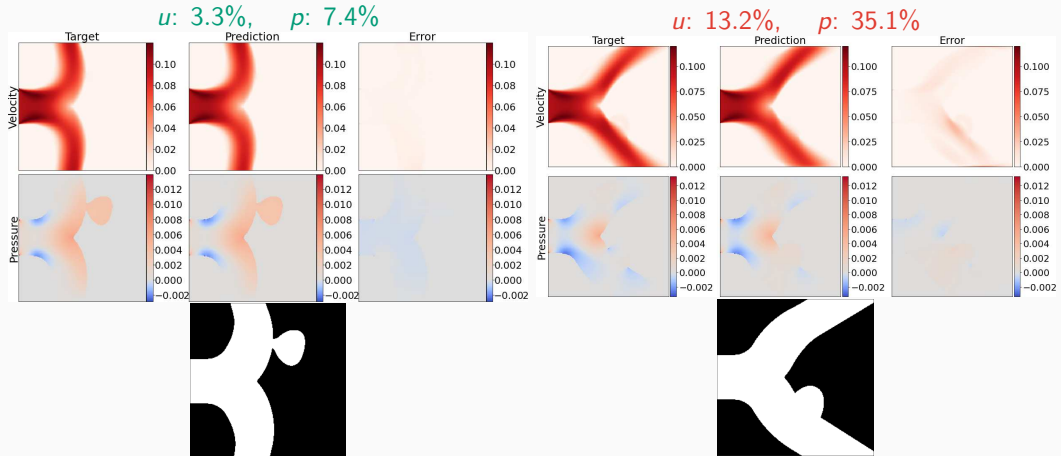
	training data	error	$\frac{\ u_{NN} - u\ _2}{\ u\ _2}$	$\frac{\ P_{NN} - P\ _2}{\ P\ _2}$	mean residual		# epochs trained
			momentum	mass			
data-based	10%	train. val.	2.07% 4.48 %	10.98% 15.20 %	$1.1 \cdot 10^{-1}$ $1.6 \cdot 10^{-1}$	$1.4 \cdot 10^0$ $1.7 \cdot 10^0$	500
	25%	train. val.	1.93% 3.49 %	8.45% 10.70 %	$9.1 \cdot 10^{-2}$ $1.2 \cdot 10^{-1}$	$1.2 \cdot 10^0$ $1.4 \cdot 10^0$	500
	50%	train. val.	1.48% 2.70 %	8.75% 10.09 %	$9.0 \cdot 10^{-2}$ $1.1 \cdot 10^{-1}$	$1.1 \cdot 10^0$ $1.2 \cdot 10^0$	500
	75%	train. val.	1.43% 2.52 %	7.30% 8.67 %	$1.0 \cdot 10^{-1}$ $1.2 \cdot 10^{-1}$	$1.5 \cdot 10^0$ $1.5 \cdot 10^0$	500
physics-informed	10%	train. val.	5.35% 6.72%	12.95% 15.39%	$3.5 \cdot 10^{-2}$ $6.7 \cdot 10^{-2}$	$7.8 \cdot 10^{-2}$ $2.0 \cdot 10^{-1}$	5 000
	25%	train. val.	5.03% 5.78 %	12.26% 13.38 %	$3.2 \cdot 10^{-2}$ $5.3 \cdot 10^{-2}$	$7.3 \cdot 10^{-2}$ $1.4 \cdot 10^{-1}$	5 000
	50%	train. val.	5.81% 5.84 %	12.92% 12.73 %	$3.9 \cdot 10^{-2}$ $4.8 \cdot 10^{-2}$	$9.3 \cdot 10^{-2}$ $1.2 \cdot 10^{-1}$	5 000
	75%	train. val.	5.03% 5.18 %	11.63% 11.60 %	$3.2 \cdot 10^{-2}$ $4.2 \cdot 10^{-2}$	$7.7 \cdot 10^{-2}$ $1.1 \cdot 10^{-1}$	5 000

→ The results for the **physics-informed approach** are **comparable to the data-based approach**; the **errors are slightly higher**. However, no **reference data at all is needed for the training**.

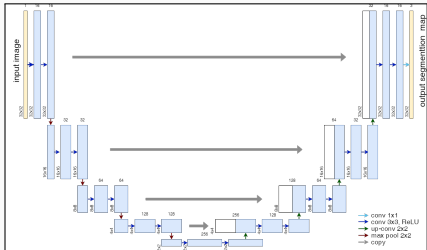
Aneurysm Geometries

Training: 500 geometries **Validation:** \approx 1200 geometries

Relative L^2 -error on the validation data set in u : 4.9 %, in p : 9.5 %.



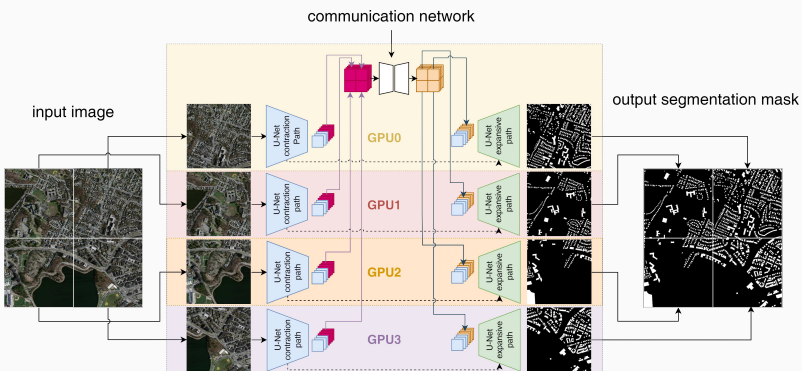
Domain Decomposition-Based U-Net Architecture



name	mem. feature maps # of values	MB	mem. weights # of values	MB
input block	268 M	1 024.0	38 848	0.148
encoder blocks	314 M	1 320	18 M	72
decoder blocks	754 M	3880	12 M	47
output block	3.1 M	12.0	195	0.001

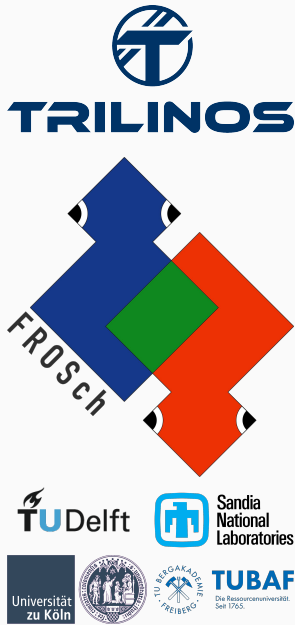
Most memory in the **U-Net** is used by **feature maps**, not weights
→ **Decompose feature maps to distribute memory consumption.**

Cf. **Verburg, Heinlein, Cyr (2025)**.



Scalable Solvers for Blood Flow Simulations

FROSch (Fast and Robust Overlapping Schwarz) Framework in Trilinos



Software

- Object-oriented C++ domain decomposition solver framework with MPI-based distributed memory parallelization
- Part of TRILINOS with the parallel linear algebra based on TPETRA
- Node-level parallelization and performance portability on CPU and GPU architectures through KOKKOS and KOKKOSKERNELS
- Accessible through unified TRILINOS solver interface STRATIMIKOS

Methodology

- Parallel scalable multi-level Schwarz domain decomposition preconditioners
- Algebraic construction based on the parallel distributed system matrix
- Extension-based coarse spaces

Team (active)

- | | |
|--|--|
| <ul style="list-style-type: none">▪ Filipe Cumaru (TU Delft)▪ Alexander Heinlein (TU Delft)▪ Kyrill Ho (UCologne)▪ Sebastian Kinnewig (LUH)▪ Axel Klawonn (UCologne)▪ Jascha Knepper (UCologne) | <ul style="list-style-type: none">▪ Stephan Köhler (TUBAF)▪ Friederike Röver (TUBAF)▪ Siva Rajamanickam (SNL)▪ Oliver Rheinbach (TUBAF)▪ Lea Saßmannshausen (UCologne)▪ Ichitaro Yamazaki (SNL) |
|--|--|

Monolithic (R)GDSW Preconditioners for CFD Simulations

Consider the discrete saddle point problem

$$\mathcal{A}x = \begin{bmatrix} K & B^\top \\ B & 0 \end{bmatrix} \begin{bmatrix} u \\ p \end{bmatrix} = \begin{bmatrix} f \\ 0 \end{bmatrix} = b.$$

Monolithic GDSW preconditioner

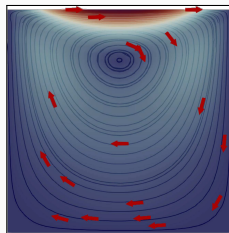
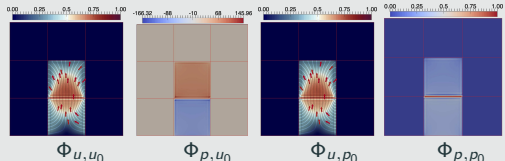
We construct a **monolithic GDSW preconditioner**

$$m_{\text{GDSW}}^{-1} = \phi \mathcal{A}_0^{-1} \phi^\top + \sum_{i=1}^N \mathcal{R}_i^\top \bar{\mathcal{P}}_i \mathcal{A}_i^{-1} \mathcal{R}_i,$$

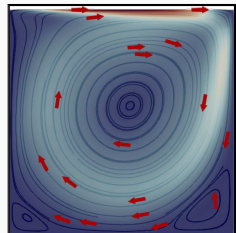
with block matrices $\mathcal{A}_0 = \phi^\top \mathcal{A} \phi$, $\mathcal{A}_i = \mathcal{R}_i \mathcal{A} \mathcal{R}_i^\top$, local pressure projections $\bar{\mathcal{P}}_i$, and

$$\mathcal{R}_i = \begin{bmatrix} \mathcal{R}_{u,i} & \mathbf{0} \\ \mathbf{0} & \mathcal{R}_{p,i} \end{bmatrix} \quad \text{and} \quad \phi = \begin{bmatrix} \Phi_{u,u_0} & \Phi_{u,p_0} \\ \Phi_{p,u_0} & \Phi_{p,p_0} \end{bmatrix}.$$

Using \mathcal{A} to compute extensions: $\phi_I = -\mathcal{A}_{II}^{-1} \mathcal{A}_{I\Gamma} \phi_\Gamma$; cf. [Heinlein, Hochmuth, Klawonn \(2019, 2020\)](#).



Stokes flow



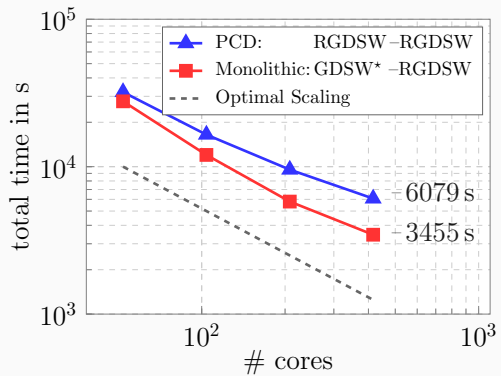
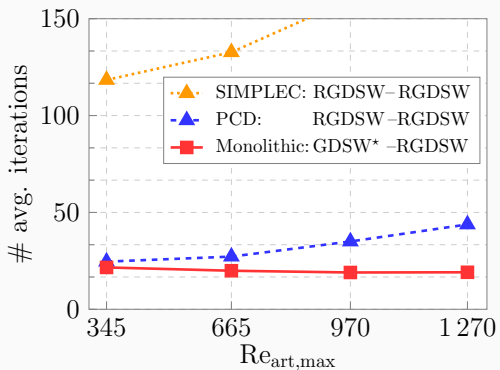
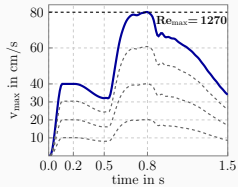
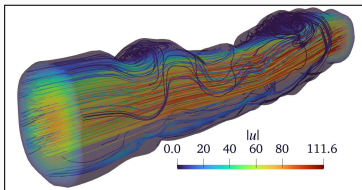
Navier–Stokes flow

Related work:

- Original work on monolithic Schwarz preconditioners: [Klawonn and Pavarino \(1998, 2000\)](#)
- Other publications on monolithic Schwarz preconditioners: e.g., [Hwang and Cai \(2006\)](#), [Barker and Cai \(2010\)](#), [Wu and Cai \(2014\)](#), and the presentation [Dohrmann \(2010\)](#) at the *Workshop on Adaptive Finite Elements and Domain Decomposition Methods* in Milan.

Results for Blood Flow Simulations

- 3D unsteady flow simulation within the geometry of a realistic artery (from [Balzani et al. \(2012\)](#)) and kinematic viscosity $\nu = 0.03 \text{ cm}^2/\text{s}$
- Parabolic inflow profile at inlet
- Time discretization: BDF-2; space discretization: P2-P1 elements



Cf. [Heinlein, Klawonn, Knepper, Saßmannshausen \(arXiv 2025\)](#)

Investigating the impact of arterial wall models

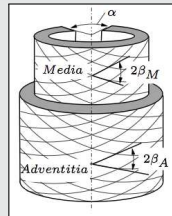
Arterial wall models

We consider **anisotropic hyperelastic material models** of the form

$$\Psi_* = \underbrace{\Psi^{\text{iso}} + \Psi^{\text{pen}}}_{\text{isotropic (neo-Hookean type)}} + \underbrace{\sum_{a=1}^2 \Psi_a^{\text{ti}}}_{\text{transversely isotropic}}$$

to account for the fibers in the arterial wall and to obtain **realistic material behavior and stresses**.

We use the material models Ψ_A , Ψ_B , Ψ_C , Ψ_D , Ψ_E , and the material parameters (**fitted to experiments**) from **Brands, Klawonn, Rheinbach, Schröder (2008)**.



Composition of the arterial wall

Monolithic solver

- We solve the **fully coupled FSI problem** using an **inexact Newton method**.
- **Monolithic block preconditioner** with a **parallel domain decomposition preconditioner** for the blocks, e.g., FROSCH.

Software framework

Trilinos (C++) LifeV (C++) FEAP (Fortran) }
Lightweight coupling library;
see **Heinlein (2016)**.

Comparing Different Material Models

We compare the material models considered in **Brands, Klawonn, Rheinbach, Schröder (2008)**.

- Model ψ_A (**Balzani, Neff, Schröder, Holzapfel (2006)**):

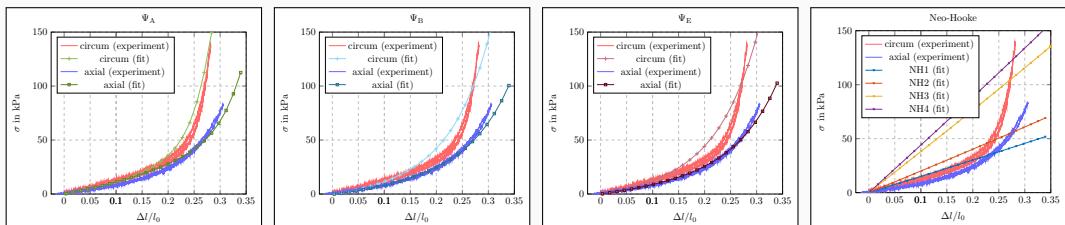
$$\psi_A = c_1 \left(\frac{l_1}{l_3^{1/3}} - 3 \right) + \varepsilon_1 \left(I_3^{\varepsilon_2} + \frac{1}{l_3^{\varepsilon_2}} - 2 \right) + \sum_{a=1}^2 \alpha_1 \left\langle I_1 J_4^{(a)} - J_5^{(a)} - 2 \right\rangle^{\alpha_2},$$

- Model ψ_B (**Holzapfel, Gasser, Ogden (2000)**):

$$\psi_B = c_1 \left(\frac{l_1}{l_3^{1/3}} - 3 \right) + \varepsilon_1 \left(I_3^{\varepsilon_2} + \frac{1}{l_3^{\varepsilon_2}} - 2 \right)^{\alpha_5} + \sum_{a=1}^2 \frac{k_1}{2k_2} \left\{ \exp \left(k_2 \left\langle \frac{J_4^{(a)}}{l_3^{1/3}} - 1 \right\rangle^2 \right) - 1 \right\}$$

- Model ψ_E (anisotropic parts: **Holzapfel, Gasser, Ogden (2004)**):

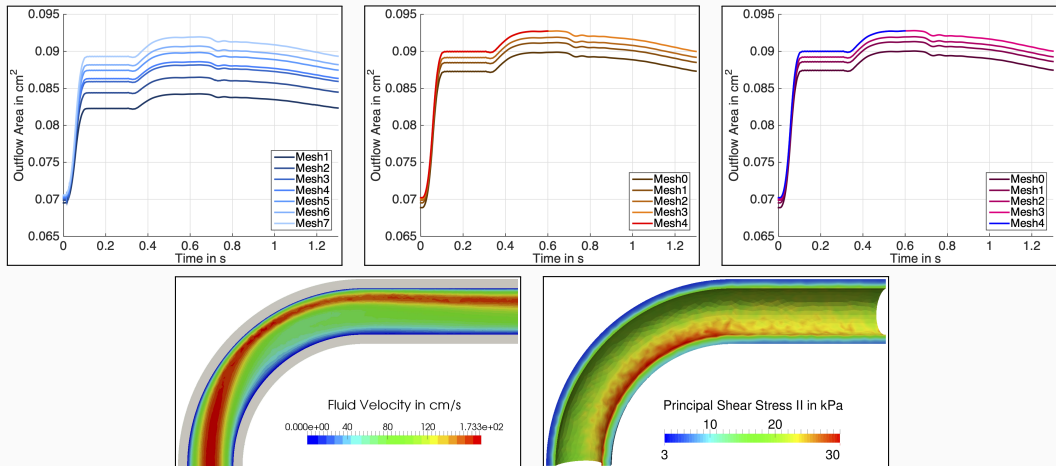
$$\psi_E = c_1 (l_1 - \ln(l_3)) + \varepsilon_1 \left(I_3^{\varepsilon_2} + \frac{1}{l_3^{\varepsilon_2}} - 2 \right) + \sum_{a=1}^2 \frac{k_1}{2k_2} \left\{ \exp \left(k_2 \left\langle J_4^{(a)} - 1 \right\rangle^2 \right) - 1 \right\}$$



Cauchy stress σ [kPa] vs. strain λ (comp) compared to the experimental data (exp).

Results Ramp & Heart Beat – Anisotropic Hyperelastic Material Model (Ψ_A)

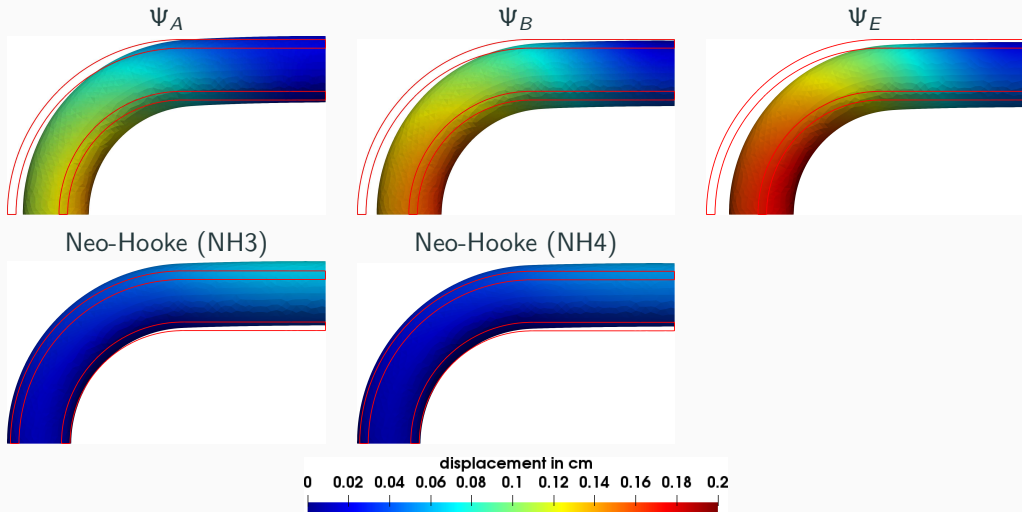
Balzani, Deparis, Fausten, Forti, Heinlein, Klawonn, Quarteroni, Rheinbach, Schröder (2016)



Top: Outflow cross sectional lumen area for P1 (left), P2 (middle), and $\bar{F} = P_2 - P_0 - P_0$ (right) elements. \Rightarrow **Mesh convergence for P2 and \bar{F} elements**

Bottom: Fluid velocities and wall stresses (left), principal shear stresses in the wall (right).

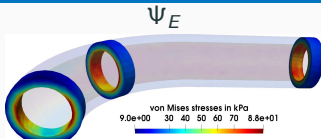
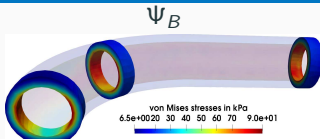
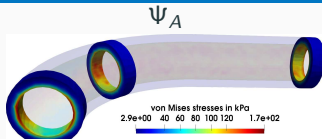
Peak Flow (0.536 s) – Structural Displacement



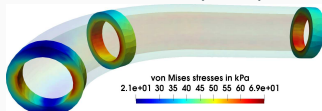
⇒ The **qualitative deformation behavior** of the neo-Hookean material model **differs significantly** from the other material models.

Cf. Balzani, Heinlein, Klawonn, Rheinbach, Schröder (2023)

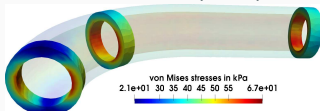
Peak Flow (0.536 s) – von Mises Stresses



Neo-Hooke (NH3)

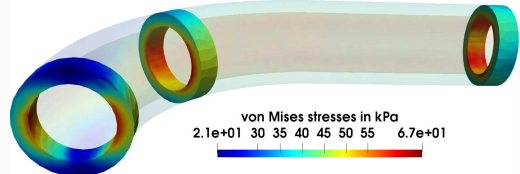
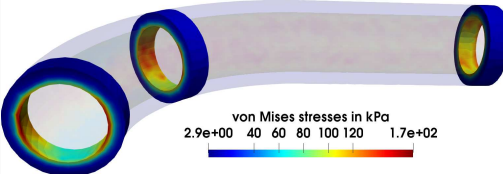


Neo-Hooke (NH4)



Ψ_A

Neo-Hooke (NH4)



⇒ Also the **qualitative stress distribution** (von Mises stresses) **differs significantly** for Neo-Hooke.

Cf. [Balzani, Heinlein, Klawonn, Rheinbach, Schröder \(2023\)](#)

Summary

Algorithmic Advances in Cardiovascular Simulations

- CNNs enable **fast surrogate models for CFD simulations**, combining data and physics for **significant prediction speedups**
- **High memory consumption** can be mitigated by employing a **domain decomposition-based U-Net architecture**
- Monolithic Schwarz preconditioners yield **scalable solvers** for **large numbers of processors** and **high Reynolds numbers**
- Fiber directions and **exponential stiffening** in the arterial wall model **strongly affect simulation outcomes**

Acknowledgements

- **Financial support:** DFG (KL2094/3-1, RH122/4-1), DFG SPP 2311 project number 465228106, Helmholtz School for Data Science in Life, Earth and Energy (HDS-LEE)
- **Computing resources:** CHEOPS (UoC), DelftBlue (TU Delft), Fritz (FAU), magnitUDE (UDE), OCuLUS (Uni Paderborn)

Thank you for your attention!